ARTICLES

Exciton-Like and Charge-Transfer States in Cyanine−Oxonol Ion Pairs. An Experimental and Theoretical Study

I. Baraldi,[†] F. Momicchioli,*[,†] G. Ponterini,[†] A. S. Tatikolov,[‡] and D. Vanossi[†]

Dipartimento di Chimica, Università di Modena e Reggio Emilia, Via Campi 183, I-41100 Modena, Italy and Institute of Chemical Physics, Academy of Sciences of Russia, Kosygin Street 4, 117977, Moscow, Russia

Received: December 13, 2000

Absorption and fluorescence emission properties of cyanine−oxonol mixed dyes, i.e., salts formed by a cationic cyanine with an anionic oxonol as counterion, were investigated both theoretically and experimentally in order to probe the effects of ion pairing occurring in low-polarity solvents. We analyzed, in particular, three model systems (S1, S2, and S3) built combining thiacarbo- and thiadicarbocyanine (C1, C2) with two vinylogous oxonol chromophores (A1/A1F, A2). In systems S1 (C1−A1) and S2 (C2−A2), where the visible absorption bands of the individual ions are almost superimposed, the formation of ion pairs gives rise to marked spectral alterations traceable to interchromophore resonance interactions. On the contrary, in system S3 (C2−A1F), whose components absorb widely apart, the spectrum of the contact ion pair and that of the dissociated form differ only for the relative band intensities. In both cases, however, contact ion pairing results in complete quenching of the emission of the chromophoric units. Such behaviors, emphasized by absorption and fluorescence emission and excitation spectra of both the mixed dyes and their components in solvents of different polarities, were the subject of a theoretical study based in particular on the calculation of structures and electronic spectra of the *contact* ion pairs. Molecular dynamics (MD) simulations and local full geometry optimizations led to two types of structures characterized by almost parallel and orthogonal arrangements of the long molecular axes. CS INDO SCI calculations using both arrangements emphasized the role of the exciton coupling between the local HOMO−LUMO excitations of the two chromophoric units. The most striking spectral characteristics in low-polarity solvent turned out to be explainable in terms of parallel type arrangements, even if an appreciable contribution of the orthogonal type structure was to be invoked for a complete interpretation of the S1 spectral properties. In all contact ion pairs, independently of the structure, the lowest excited singlet is a forbidden anion → cation charge transfer (CT) state explaining why no fluorescence emission was observed in such systems.

1. Introduction

Cyanine-type dyes have attracted much attention since the discovery of their capability of spectrally sensitizing silver halides (Vogel, 1873)[1] and, in the past decades, have become the object of renewed interest for their employment in a number of innovative applications (e.g., in dye lasers,[2] optically nonlinear devices,[3] organic dye-sensitized solar cells,[4] artificial antenna systems,[5] etc.). They include a great variety of dyes whose primary chromophores can be schematized by the formula $X-(CH)_n-X'$, where $n = 1, 3, 5, ...$, and X, $X' = NR_2$, O. The symmetric systems, $X = X' = NR_2$ and $X = X' = O$, form the primary chromophores of (cationic) cyanines and (anionic) oxonols, while the asymmetric combination of the terminal groups yields the primary chromophore of (neutral) merocyanines (neutrocyanines).[1,6,7] All of the three chromophores bear $(n + 3)$ π-electrons and are basically similar to the iso-π-electronic carbanions $[CH_2-(CH)_n-CH_2]^-$.[7]

Following previous extensive -both theoretical and experimental- work on spectroscopic and photochemical properties of cyanines[8,9] and merocyanines[10] in solution, recently we turned to the study of the spectral modifications induced by H and J aggregation in merocyanines[11] and to the influence of ion pair formation on spectra and photochemistry of cationic cyanines in low polarity solvents.[12−14]

The latter papers dealt with ion pairing effects in salts of symmetric and asymmetric cationic cyanines with simple colorless counterions (I^-, Cl^-, and ClO_4^-) and the alterations of spectra and cis−trans photoisomerization dynamics observed in low polarity media were interpreted in terms of location of the anions in the contact ion pairs. Interestingly, still greater alterations of spectroscopic and photophysical properties have been reported for cation−anion dyes,[15] i.e., salts formed by a cationic cyanine with an anionic polymethine dye as counterion. Particularly marked alterations of position and shape of the electronic bands, with respect to those observed in high polarity solvents, were found with cationic and anionic dyes absorbing in the same regions. Such experimental findings stimulated us to probe the subject more deeply by carrying out a new experimental inves-

* Corresponding author. Phone: 0039 59 2055081. Fax: 0039 59 373543. E-mail: momicchioli.fabio@unimo.it.
[†] Università di Modena e Reggio Emilia.
[‡] Academy of Sciences of Russia.

10.1021/jp004479t CCC: $20.00
Published on Web 04/21/2001

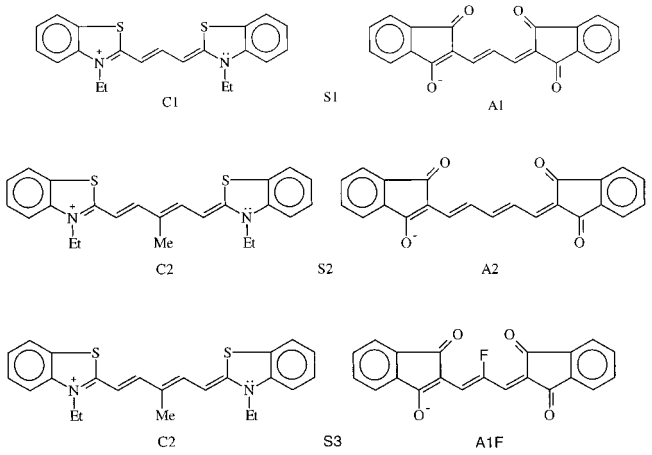

Figure 1. Structural formulas of the cations (C1 and C2) and anions (A1, A2, and A1F) forming the three investigated cyanine-oxonol dyes (S1, S2, and S3).

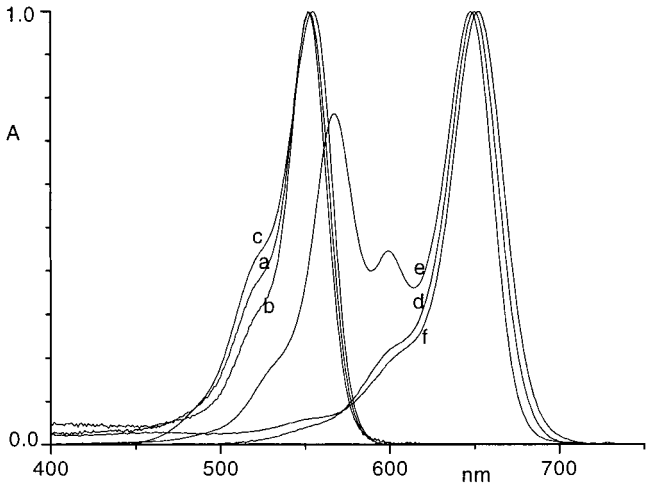

Figure 2. Normalized absorption spectra in acetonitrile: S1 (a), A1TC (b), C1I (c), S2 (d), S3 (e), and A2TA (f).

tigation, combined with a thorough theoretical study, on a selected set of three cyanine-oxonol dyes (Figure 1).

Except for the F substitution at the central carbon atom of A1F, the three mixed dyes are none other than three of the four binary systems that can be formed with two cyanine cations (C1 and C2) and two oxonol anions (A1/A1F and A2). The components of S1 (C1 and A1) derive from the cyanine and oxonol primary chromophores with $n = 5$ and $n = 7$, respectively, which are known to have strongly overlapping absorption bands in the 400−450 nm region.[16] In the same way, the components of S2 (C2 and A2), bear the cyanine and oxonol primary chromophores with $n = 7$ and $n = 9$, which exhibit nearby absorption bands ∼100 nm to the red of the corresponding bands of the C1 and A1 chromophores. On the other hand, in the case of the S3 (C2−A1F) system the absorption regions of the cationic and anionic primary chromophores are quite far apart. These basic features and additional effects due to incorporation of the chromophore terminations in proper heterocyclic groups (Figure 1) cause the color bands of C1 and A1, as well as those of C2 and A2, to be almost superimposed, while C2 and A1F, i.e., the components of the S3 system, retain widely apart absorptions. Thus, in S1 and S2 mixed dyes ionic pairing occurring in little polar solvents should result in strong interchromophore resonance interactions and hence in marked spectral alterations. In the S3 system, on the other hand, the formation of ion pairs is expected to give rise to negligible resonance interactions so that its absorption spectrum should be scarcely affected by changes in solvent polarity, apart from minor solvatochromic shifts.

Taking the three cyanine-oxonol dyes of Figure 1 as suitable test systems, with the present work we aimed at establishing the most probable ion pair structures and interpreting their absorption and emission properties in terms of interchromophore interactions. The absorption spectra of the three mixed dyes and of the salts formed by the individual cationic and anionic chromophores with colorless counterions, were first measured in solvents of very different polarities. A parallel investigation was carried out on the fluorescence properties including emission and excitation spectra as well as florescence quantum yields. Experiments provided clear evidence to conclude that the striking spectral features observed in low-polarity solvents are due to formation of *contact* ion pairs, while involvement of other aggregation types can be ruled out. On this basis we performed a theoretical study on structures and electronic spectra of the separate ionic species (C1, C2, A1, A1F, and A2) and of the contact ion pairs corresponding to the S1, S2, and S3 mixed systems. The more stable minima on the ion-pair potential-energy-surfaces (PES) were localized by molecular dynamics (MD) calculations using the classical MM+ force field[17] and the geometries of the so determined spatial arrangements were then optimized at the PM3 level.[18] The latter local procedure was also used to determine the geometries of the individual chromophores. At last, using these geometries the electronic spectra of both ion pairs and separate ionic dyes were calculated by the CS INDO CI method.[19] The calculation results provided a satisfactory general explanation of the experimental observations emphasizing, in particular, the role of exciton-like and charge transfer states occurring in contact ion pairs.

2. Experimental Study

2.1. Absorption Spectra of the Solvated Ions. The absorption spectra of S1 and of the salts formed by its anion with a simple trimethine cyanine ($(H_3C)_2-N-(CH)_3-N-(CH_3)_2^+$, TC) and its cation with I^- (A1TC and C1I, respectively) were first measured in acetonitrile, a polar dissociating solvent, so as to observe the relative positions of the color bands of the two chromogens in the absence of a significant interaction between ions (Figure 2, curves a−c). In this solvent, the lowest energy bands of A1 and C1 were almost superimposed: the maxima coincided within 3 nm (552 and 555 nm, respectively) and the bandwidths of the three salts were almost the same. Similarly, the spectra of S2, S3 and the salt formed by A2 with $NH(CH_2CH_3)_3^+$ (TA) as the counterion (A2TA) in acetonitrile showed almost superimposed lowest energy bands (Figure 2, curves d−f). Maxima were found at 648 nm for S3 (corresponding to the C2 absorption), 652 nm for A2 and 650 nm for the composite dye, S2. Again, the bandwidths were very similar to each other. The spectrum of S3 differed qualitatively from the other two in the region between 500 and 620 nm, due to the presence of the color band of A1F, whose maximum lied at 568 nm, and of the second vibronic band of C2 which, because of its overlapping with the absorption of A1F, was unusually pronounced and featured a maximum at 599 nm. For all dyes, much weaker bands, corresponding to higher energy transitions, were observed in the near-UV region (see Table 1 for relevant spectral properties). To sum up, while S1 and S2 are composed of ions having almost equal (S_0-S_1) transition energies, A1TC, C1I, and A2TA each contain only one visible-absorbing dye and, finally, S3 contains two dyes whose color bands are separated by about 2200 cm^{-1}. Comparison of the spectral

TABLE 1: Comparison between Calculated S_0-S_n ($n = 1, 2, 3$) Transitions and Experimental Spectra of C1 and C2

		CS INDO SCI			experimental results[a]	
dye	transition	ΔE (eV)	f	major excited-state configurations	ΔE (eV)	$10^{-5}\epsilon_{max}$
C1	S_0-S_1	2.60	1.474	[H,L] (94%)	2.23	1.5 ($f = 1.1$)
	S_0-S_2	3.86	0.034	[H-1,L] (89%)	3.87	sh
	S_0-S_3	4.16	0.055	[H-3,L] (87%)	4.17	0.16
C2	S_0-S_1	2.28	1.975	[H,L] (93%)	1.91	2.3 ($f = 1.3$)
	S_0-S_2	3.63	0.052	[H-1,L] (87%)	3.50	sh
	S_0-S_3	4.14	0.057	[H-2,L] (48%), [H-3,L] (34%)	3.77	0.14

[a] In acetonitrile. Estimated errors in ϵ_{max} and f: ±10%.

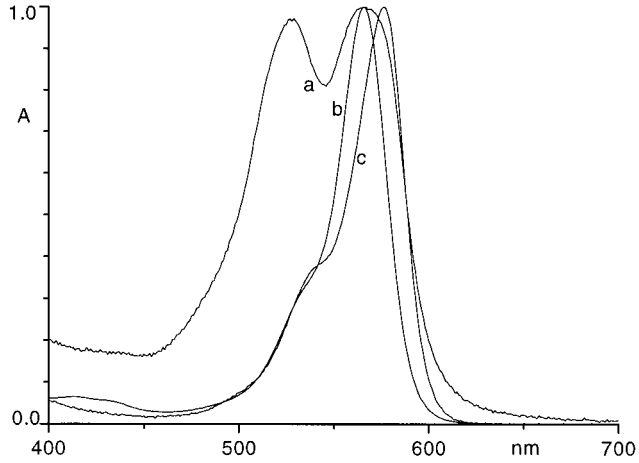

Figure 3. Normalized absorption spectra in toluene: S1 (a), A1TC (b), and C1I (c).

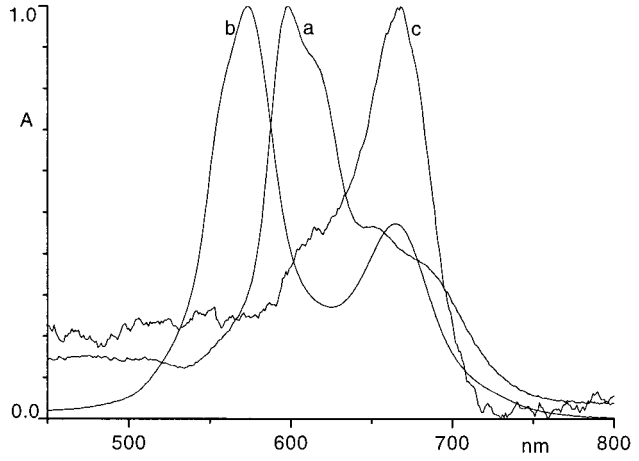

Figure 4. Normalized absorption spectra in toluene: S2 (a), S3 (b), and A2TA (c).

behaviors of S1 and S2 with those of the corresponding salts containing dyes with noncoincident absorptions will therefore highlight the consequences of such spectral coincidence in conditions where the two oppositely charged ions can interact, i.e., in contact ion pairs obtained in a low-polarity associating solvent, such as toluene. With reference to their peculiar spectral features, S1 and S2 contact ion pairs will hereafter be denominated resonant to distinguish them from S3, A1TC, C1I and A2TA contact ion pairs characterized by negligible interionic resonant interactions. The validity of this denomination will be theoretically confirmed in section 3.

2.2. Absorption Spectra of the Ion Pairs. The color bands of the nonresonant ion pairs A1TC and C1I in toluene (Figure 3, curves b and c) were characterized by shapes similar to those found in acetonitrile and usual for cyanine dyes. They exhibited slight bathochromic shifts with respect to their positions in the polar solvent in keeping with the negative solvatochromism of most polymethinecyanines: their maxima were found, respectively, at 565 and 576 nm, i.e., they were red-shifted by 416 and 650 cm^{-1}. The absorption spectrum of the resonant ion pair S1 (Figure 3, curve a) was, instead, deeply modified with respect to the spectrum of S1 in acetonitrile. It consisted of two bands with maxima at 566 and 527 nm and similar intensities. The first one lay in the absorption region of the two nonresonant ion pairs but was much broader than those bands and had a tail that extended to about 660 nm. The second one was new and peculiar to this ion pair.

The nonresonant ion pairs corresponding to S2, i.e., A2TA and S3, behaved in toluene similarly to the nonresonant ion pairs of S1. In the visible spectral region, they exhibited absorption bands corresponding to those observed in acetonitrile, with maxima at 668 nm (A2TA) and 664 and 573 nm (S3) (see Figure 4, curves b and c). So, solvatochromic and ion-pairing effects caused a bathochromic shift of both A2 and C2 bands of 370 cm^{-1} with respect to their positions in the polar solvent. As far as band shape is concerned, a pronounced change was observed in the relative intensities of the C2 and A1F bands: while the former was higher than the latter in acetonitrile, the opposite occurred in toluene. Also, the A1F band was broader and had a more pronounced shoulder in toluene than in acetonitrile. However, it was the resonant ion pair S2 that exhibited the most peculiar spectrum in toluene (Figure 4, curve a). In the visible region this was characterized by a new, intense band with a maximum at 598 nm, a steep edge to the blue and a high shoulder to the red, around 610 nm. A broad and wavy shoulder was observed in the region of the color band in acetonitrile, i.e., around 650 nm, with a tail extending to about 780 nm.

The peculiar spectral characteristics of the resonant ion pairs S1 and S2 were not due to any special ability of these salts to form ion-pair aggregates in toluene. This was shown by two different sets of experiments. In the first one, we added small amounts of acetonitrile to toluene solutions of both salts. The consequence was a gradual change of the absorption spectra from those characteristic of the first to those observed in the second solvent, with isosbestic points fairly well preserved, as long as dilution effects remained low, at about 550 and 630 nm, respectively. This indicates that only two species were involved in the equilibria whose positions were affected by the binary solvent composition. That neither of these species was an ion-pair aggregate was demonstrated by dilution experiments: the essential spectral features of S1 and S2 in toluene were not modified after dilution with the same solvent by factors 1:32 and 1:64, respectively (concentrations were, typically, between 10^{-6} and 10^{-8} mol L^{-1}).

2.3. Fluorescence Properties of Solvated Ions and Ion Pairs. All six salts investigated exhibited regular fluorescence spectra in acetonitrile. As an example, the spectra of S1 are displayed in Figure 5. In all cases, we observed coincidence of the absorption and excitation bands. The emission spectra

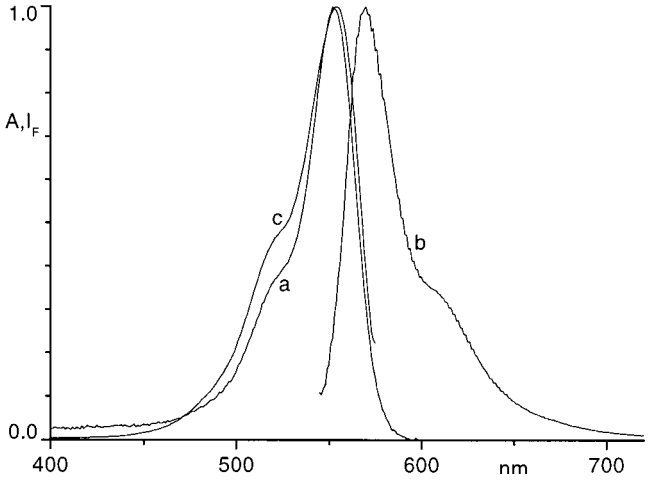

Figure 5. Normalized spectra of S1 in acetonitrile: absorption (a), emission (b, $\lambda_{exc} = 540$ nm), excitation (c, $\lambda_{obs} = 580$ nm).

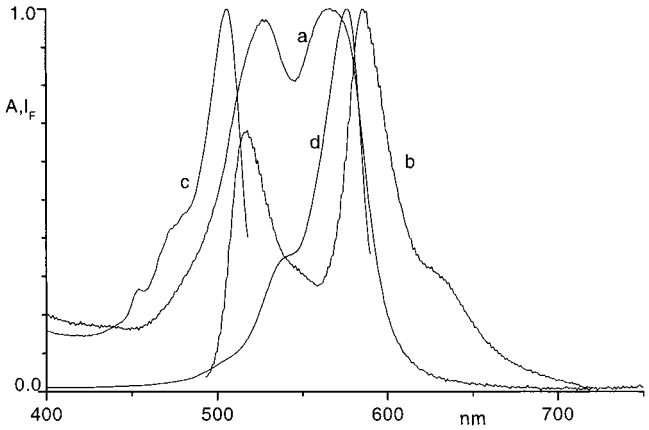

Figure 6. Normalized spectra of S1 in toluene: absorption (a), emission (b, $\lambda_{exc} = 485$ nm), excitation (c, $\lambda_{obs} = 525$ nm; d, $\lambda_{obs} = 595$ nm).

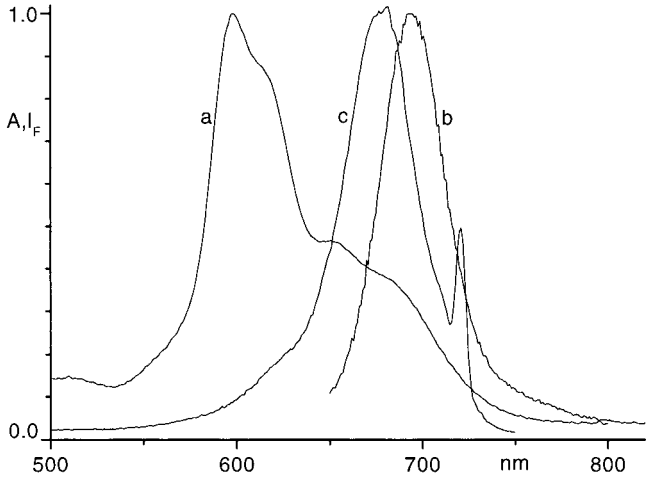

Figure 7. Normalized spectra of S2 in toluene: absorption (a), emission (b, $\lambda_{exc} = 645$ nm), excitation (c, $\lambda_{obs} = 720$).

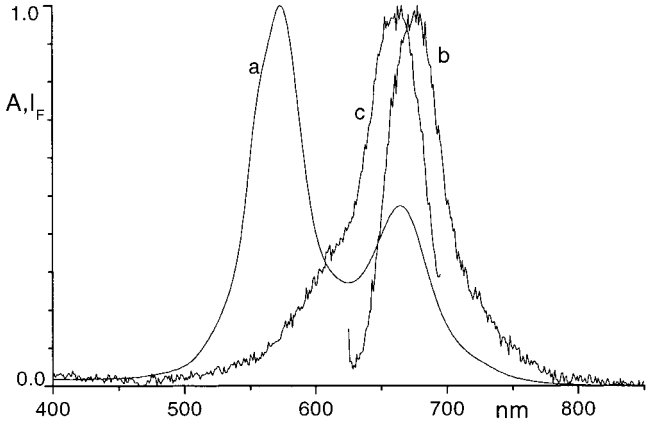

Figure 8. Normalized spectra of S3 in toluene: absorption (a), emission (b, $\lambda_{exc} = 620$ nm), excitation (c, $\lambda_{obs} = 700$ nm).

showed a quite good mirror relationship with the absorption spectra and the Stokes shifts were rather small, from 370 to 570 cm^{-1}. These characteristics are usual for polymethinecyanines and suggest that only minor structural changes take place in the S_1 state of the solvated dye, relative to the S_0 state, during the fluorescence lifetime. The emission spectra of both S1 and S2 were essentially independent of the excitation wavelength, thereby confirming the almost exact superposition of the absorption bands of their component ions. Fluorescence quantum yields were only determined for S2 and its two nonresonant partners (A2TA and S3). These held 0.03 (±0.005) and 0.20 (±0.06) for the oxonol A2 and the cyanine C2, respectively, the uncertainty of the latter value being increased by the partial spectral overlap of the fluorophore with its counterion A1F. Quite reasonably, S2 exhibited an intermediate quantum yield in acetonitrile, i.e., 0.12 (±0.03). In keeping with the previous observation, this was independent of the excitation wavelength, therefore suggesting an equipartition of the absorbed photons between the two chromophores having superimposed absorptions.

The fluorescence emission spectrum of S1 in toluene, shown in Figure 6 , curve b, together with the excitation (curves c and d) and absorption (curve a) spectra, featured two bands with maxima at 515 and 586 nm. The excitation spectrum of the first one was found in a region (maximum at 505 nm) where no significant absorption feature was observed: we attribute it to a highly fluorescent impurity well dissolved by toluene (it was not observed in acetonitrile). The second emission was only slightly blue-shifted with respect to the emission of C1I in toluene (maximum at 588 nm), while the two corresponding excitation spectra coincided both in position (maximum at 576 nm) and shape (apart from the expected inner filter effect between 500 and 570 nm in the case of S1). The mentioned excitation spectrum, however, corresponded to only a shoulder in the broad absorption band of S1 in toluene with maximum at 566 nm. The relative intensity of this shoulder was rather variable from sample to sample and increased slightly with dilution. We suggest it is due to a small, variable amount of solvent-separated ion pairs of S1. In fact, because of the absence of direct anion−cation interaction, such a species is expected to exhibit absorption and fluorescence properties similar to those of the nonresonant contact ion pairs and, apart from solvatochromic effects, of the solvated ions of S1 in acetonitrile. So, we conclude that neither of the two observed fluorescent species is responsible for the main features of the absorption spectrum of the S1 contact ion pair in toluene.

The same conclusion holds for S2 in this solvent, based on similar observations. Here, only one fluorescent species was observed with spectra, shown in Figure 7, very similar to those of A2TA in toluene and, therefore, attributed to solvent-separated ion pairs. Again, the excitation spectrum did not reproduce any of the absorption bands. Because of this discrepancy, a measurement of the quantum yield of this emission would have been unreliable and of little significance.

The fluorescence spectra in toluene of the nonresonant ion pairs S3 (shown as an example in Figure 8), C1I, A1TC, and

A2TA exhibited coincidence of the excitation and absorption bands (that of C2 for S3) and mirror relationship between absorption and emission. The emission maxima were bathochromically shifted by 400−500 cm^{-1} relative to their positions in acetonitrile: solvatochromic and ion pairing effects were quite the same as for absorption. The emissions in toluene were weaker than in acetonitrile. So, for A2TA, the quantum yield was 8 (±3) × 10^{-3}, i.e., about 4 times smaller than that for A2 in acetonitrile, and for S3 the quantum yield measured upon excitation in the absorption region of the cation was only of the order of 1 × 10^{-3}, i.e., more than 2 orders of magnitude lower than that found for C2 in acetonitrile, and showed poor reproducibility from sample to sample. These observations suggest that the emission of S3 in toluene originates from residual solvent-separated ion pairs, while contact ion pairs are nonfluorescent, in analogy with S1 and S2.

To sum up, the formation of contact ion pairs has qualitatively different effects on the absorption properties of the investigated salts, depending on whether the solvated anion and cation have superimposed absorptions in acetonitrile. While regular bands with shapes typical of cyanine dyes are observed in the latter case, unusual spectra exhibiting a new intense band to the blue of the normal color band with several shoulders and an absorption tail slowly decreasing to the red are obtained in the former case. The two conditions necessary for these spectroscopic peculiarities to show up, i.e., contact ion pairing and superimposed lowest-energy absorptions, suggest exciton interaction between the two oppositely charged chromophores to be operative in contact ion pairs (see section 3). As far as fluorescence properties are concerned, on the other hand, the investigated salts are similar to each other: regular emission and excitation bands are observed in all cases, even though weaker than in acetonitrile and, in the cases of S1, S2, and S3, attributable to residual solvent-separated ion pairs. A common peculiar characteristic of these contact ion pairs is that they are not fluorescent.

Experimental Section

The dyes A1TC, A2TA, S1, S2, and S3 were given to us by Dr. Zh. A. Krasnaya (Moscow). The synthesis of A1TC and A2TA is described in ref 20, and that of S3 in ref 21. The resonant dyes S1 and S2 have been synthesized similarly to the latter. C1I was obtained from Merck. Acetonitrile (LABSCAN) was used as received, while toluene (Merck) was dehydrated with activated molecular sieves. Absorption spectra were measured with a Perkin-Elmer Lambda 15 spectrophotometer. Fluorescence spectra were obtained from a Jobin Yvon-Spex Fluoromax 2 fluorometer and were corrected for the instrumental spectral sensitivity. Fluorescence quantum yields were determined relative to cresyl violet perchlorate in methanol (7.5×10^{-7} mol L^{-1}; $\Phi_F = 0.67$[22]).

3. Theoretical Study of Individual Ionic Dyes and Contact Ion Pairs

The theoretical study that follows aims at providing as consistent an explanation as possible of the peculiar absorption-emission properties of S1, S2, and S3 mixed dyes as have emerged from the spectroscopic investigation of the previous section. We will try, in particular, to find out the origin of the most striking spectral modifications observed on changing from acetonitrile to toluene solutions. To make the problem easier, we assumed the spectroscopic properties in acetonitrile and toluene to be due only to the separated ions and the contact ion pairs, respectively. Moreover, we neglected the observed slight solvatochromic effects, so calculations of structures and electronic spectra were limited to unsolvated ions and ion pairs.

3.1. Calculation Procedures. *3.1.1. Structures of Ions and Ion Pairs.* Structure calculations were entirely performed using the HyperChem computational package.[17] The structures of the individual chromophores were calculated by full geometry optimization at the semiempirical PM3 SCF level using the gradient Polak−Ribiere procedure.

The structures of the contact ion pairs, on the other hand, were derived from a more complex procedure combining (i) exploration of the potential energy surface (PES) by classical molecular dynamics (MD) simulations and (ii) local geometry optimizations by both molecular mechanics (MM) and semiempirical quantum mechanical calculations.

To be more precise, in step i, potential energy calculations were carried out by the MM method using the HyperChem MM+ force field.[17] The atomic charges needed to evaluate the nonbonded electrostatic interactions were obtained by PM3 SCF calculations on the individual ions. Using this MM/MM+ approach, we optimized first of all the geometries of the two separate dyes and then those of a set of ion pairs corresponding to arbitrarily fixed arrangements of the subunits. Such geometries were the starting structures of as many 5 ps real-time simulations of the ion pair dynamics subjected to the MM+ force field, from which the main attractive regions of the PES were singled out. In step ii, the geometries of the so localized configurations were optimized again at the MM/MM+ level and were finally refined by full optimization at the PM3 SCF level.

3.1.2. Electronic Spectra. The optimized geometries of the individual ionic dyes (C1, C2, A1, A1F, and A2) and of the contact ion pairs (S1, S2, S3) were used to calculate the electronic spectra in the isolated molecule approximation. In both cases, calculations were based on the CS INDO Hamiltonian[19] which has proved to be an efficient tool for dealing with spectroscopic and photochemical properties of large conjugated systems such as the cyanine dyes under study.[8−10]

Standard delocalized CS INDO CI calculations were carried out for the individual ions as well as for the ion-pair systems. In short, we recall that the CS INDO method uses a basis set of hybrid AOs of the σ, π, and n type, derived from pure Slater AOs by Del Re's automatic procedure[23,24] and makes the resonance integrals $\beta_{\mu\nu}$ to depend on the "chemical" nature of the interacting orbitals by the introduction of proper screening factors ($k_{\sigma\sigma}$, $k_{\sigma\pi}$, $k_{\pi\pi}$, etc.). Moreover, the electron repulsion integrals γ_{AB} are evaluated according to one of the current "spectroscopic" parametrizations (Ohno−Klopman, Mataga−Nishimoto) and the core−core repulsions (E_{AB}^{CR}) are obtained by a formula self-fitting the adopted γ_{AB} functions. Finally the SCF calculations are completed by a proper CI treatment, the extension of which has to be fixed with relation to the adopted parametrization of $\beta_{\mu\nu}$ and γ_{AB} integrals as well as to the goal set.

In the present work the orbital hybridization was performed starting from the Slater s and p valence set for both the first row atoms (2s and 2p) and the sulfur atom (3s and 3p) of the cationic cyanines (C1 and C2), the involvement of the sulfur 3d orbitals being negligible a priori in view of the low valence state of the S atom in such systems. The screening factors entering the $\beta_{\mu\nu}$ integrals were given the values: $k_{\sigma\sigma} = 1$, $k_{\sigma\pi} = 0.65$, $k_{\pi\pi} = 0.50$, $k_{n\sigma} = 0.72$, $k_{n\pi} = 0.60$, $k_{nn} = 0.68$,[9b] and γ_{AB} integrals were calculated by the Mataga−Nishimoto (MN) formula.[25] All other parameters were given the same values as in ref 9b. The CI treatments were limited to the singly excited

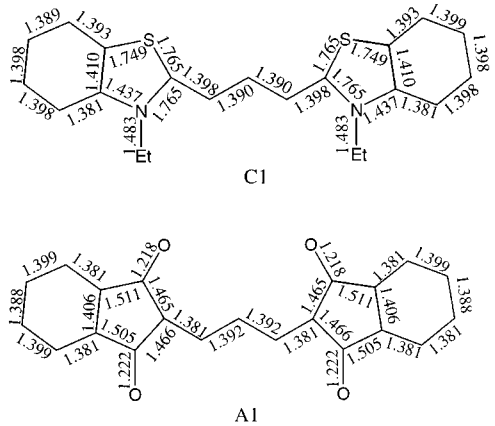

Figure 9. Bond lengths of dyes C1 and A1 obtained from full geometry optimization with PM3 method.

configurations (SCI). As previously pointed out,[19] the MN SCI version of the CS INDO method (with $k_{\pi\pi} = 0.5$) can provide fairly good excited-state descriptions at least as regards the lowest lying excited singlet states of the $\pi\pi^*$ type. Thus, the adopted CI and parametrization appear to be right for our purpose, since the spectra under study (Figures 2−8) are essentially due to one-electron transitions from HOMOs to LUMOs of the involved ionic dyes. The SCI calculations were expanded on a limited, yet fairly large, basis of highest occupied and lowest virtual π MOs. Precisely, the active-space π MOs (occupied + virtual) were 14−16 for the individual chromophores and 28−30 for the contact ion pairs.

3.2. Results and Discussion. *3.2.1. Structures and Electronic Spectra of Individual Dyes*. From the full geometry optimization at the PM3 level, all the dyes under study (C1, C2, A1, A1F, and A2) were found to be planar (except for the substituent groups Me and Et) and have all-trans configuration. As was expected for symmetrical cyanine dyes, the C−C bonds belonging to the central polymethine chain were found to have very similar lengths. Such characteristics are illustrated in Figure 9 where the calculated structures of C1 and A1 are given as an example.

Using the optimized geometries, the electronic spectra of the five dyes were then calculated by the CS INDO CI method. The calculation results (energy ΔE, oscillator strength f, and excited-state nature) concerning the first three S_0-S_n transitions of the cations (C1 and C2) and the anions (A1, A1F, and A2) are collected in Tables 1 and 2, respectively, together with the relevant spectral data obtained in acetonitrile solution.

First, it can be noted that the energy of the first electronic transition is systematically overestimated by ∼0.4 eV. As has been shown in previous papers on electronic spectra and photoisomerism of strepto- and carbo-cyanines (C1 included)[9] such general overestimation is due to limitation of the CI to singly excited configurations, even if the effect is mitigated by the use of MN repulsion integrals. Apart from that, in all dyes under study the color band is mainly attributable to the one-electron excitation from the HOMO (H) to the LUMO (L) essentially localized on the respective (cyanine/oxonol) primary chromophore (for an analysis of the MO basis set in terms of relevant molecular subunits, see ref 9b). However, the behavior of the cations (Table 1) and that of the anions (Table 2) are rather different as far as origin and location of the immediately upper excited singlets are concerned. As a matter of fact, the S_0-S_2 and S_0-S_3 transitions of C1 and C2 appear to have a substituent → chromophore CT character (the starting H−1, H−2 and H−3 orbitals being localized on the terminal benzene rings) and are predicted to give rise to the weak UV-absorption regions with maxima at 4.17 and 3.77 eV, respectively (see also ref 9b). On the contrary, the S_0-S_2 and S_0-S_3 transitions of A1, A1F, and A2 have reverse chromophore → substituent CT character (the L+1 and L+2 orbitals being localized on the terminal groups). In A1 (A1F) such transitions are predicted to have medium/low intensity and to lie right next to the H−L transition so that they should be hidden by the intense color band. In A2 both S_0-S_2 and S_0-S_3 transitions have low intensity ($f < 0.1$), and according to the calculated relative energies, they should lie under the tail to the blue of the color band.

Finally, the results of Tables 1 and 2 emphasize two good general characteristics of the CS INDO SCI results concerning the lowest wavelength transition. First of all, the reduction in transition energy observed on passing from C1, A1 to C2, A2 (corresponding to the so-called 100 nm "vinylene shift" of symmetrical polymethines[6]) is well reproduced by calculations. Second, C1 and A1, as well C2 and A2, are predicted to have almost equal transition energies in very good agreement with experiment. The latter is quite an important result since it represents a necessary condition in order that the peculiar spectroscopic properties exhibited by the C1/A1 and C2/A2 contact ion pairs may be theoretically accounted for.

3.2.2. Structures and Electronic Spectra of S1, S2, and S3 Contact Ion Pairs. MD simulations and local geometry optimizations according to the procedure outlined in section 3.1.1, led systematically to two types of stable ion-pair structures like those shown by way of example in Figure 10 for the pair S1.

In the structures of the **a** type both the long axes and the molecular planes of the chromophores are almost parallel to each other, while **b** type structures are characterized by an almost perpendicular arrangement of the long axes and by appreciably nonparallel molecular planes. In the case of S1, MD simulations led to **a** and **b** type structures with about the same probability, while **a** type and **b** type structures were prevailingly obtained for S2 and S3, respectively. The average distance between the molecular planes was found to be between 3.4 and 3.6 Å in S1 and S2, and about 4 Å in S3.

Interestingly, the prediction of an equi-probable occurrence of **a** and **b** type arrangements in the S1 ion pair is in keeping with the crystal structures of two polymorphs formed by the 3,3′-dimethylthiacarbocyanine (differing from C1 only for methyl instead of ethyl substitution) and an oxonol bearing the same primary chromophore as A1.[26] As a matter of fact, X-ray crystallography of the two polymorphs showed that the long molecular axes of the ions were parallel in one case and nearly orthogonal in the other, the closest interaction distances being 3.3 and 3.2 Å, respectively.

To gain an insight into the stabilities of the so determined structures we estimated in each case the interion interaction energy (E_{int}) as the difference between the energy of the contact ion pair and that of the two ions infinitely far from each other. The calculations were carried out at the PM3 level and interaction energies ranging from ∼ −200 to −250 kJ mol^{-1} were found. Leaving out secondary effects due to the so-called basis set superposition error (BSSE),[27] qualitatively speaking it is to be noted that the calculated interaction energies are over five times those recently reported for two dimeric forms of a neutral cyanine dye (merocyanine) (≤40 kJ mol^{-1}).[11] Clearly, this result is in keeping with the stabilization energy of the systems under study being primarily due to electrostatic interaction between the oppositely charged components. This was verified by calculating the charge−charge interaction energy by the equation

TABLE 2: Comparison between Calculated S_0-S_n ($n = 1, 2, 3$) Transitions and Experimental Spectra of A1, A1F, and A2

		CS INDO SCI			experimental results[a]	
dye	transition	ΔE (eV)	f	major excited-state configurations	ΔE (eV)	$10^{-5}\epsilon_{max}$
A1	S_0-S_1	2.69	1.322	[H,L] (83%)		
	S_0-S_2	2.85	0.101	[H,L+2] (81%)	2.25	1.7 ($f = 1.0$)
	S_0-S_3	2.86	0.173	[H,L+1] (79%)		
A1F	S_0-S_1	2.66	1.487	[H,L] (72%)		
	S_0-S_2	2.74	0.207	[H,L+2] (69%)	2.18	1.6 ($f = 1.0$)
	S_0-S_3	2.75	0.085	[H,L+1] (92%)		
A2	S_0-S_1	2.32	2.032	[H,L] (94%)		
	S_0-S_2	2.65	0.089	[H,L+1] (89%)	1.90	1.8 ($f = 1.2$)
	S_0-S_3	2.82	0.040	[H,L+2] (91%)		

[a] In acetonitrile. Estimated errors in ϵ_{max} and f: ±15%.

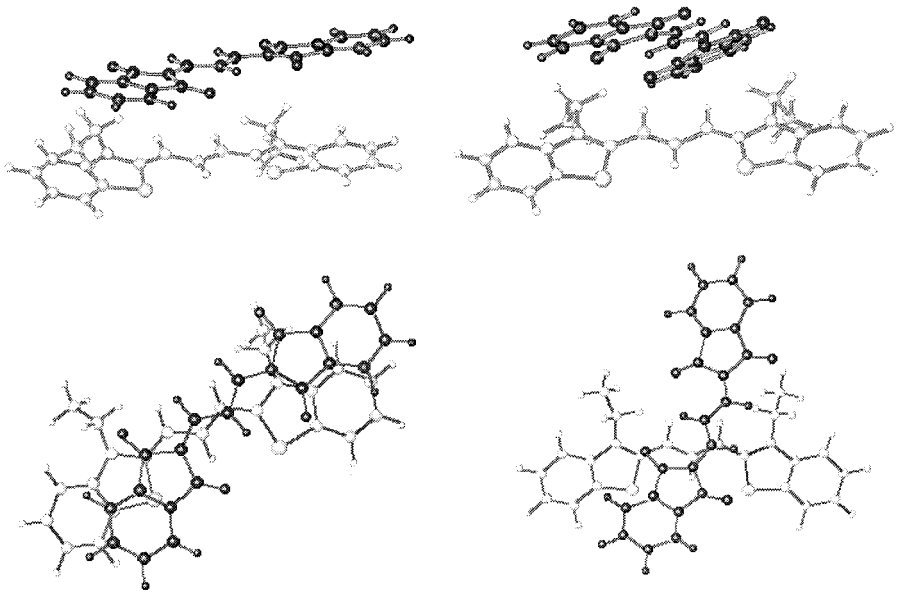

a **b**

Figure 10. Parallel (**a**) and orthogonal (**b**) type arrangements for S1 contact ion pair (the atoms of the anion are in black). The bottom and top representations emphasize the orientations of the long molecular axes and those of the molecular planes, respectively.

$$E_{int}^{ch} = \sum_{r\in C}\sum_{s\in A}\frac{q_r q_s}{R_{rs}} \quad (1)$$

where R_{rs} is the distance between the atom r (of the cation) and the atom s (of the anion) and q_r (q_s) are the (PM3) net atomic charges. According to the Claverie's decomposition of the overall interaction energy,[28] eq 1 can be seen as the first term of a multipolar multicentric development of the total electrostatic energy (E_{int}^{elec}). As expected E_{int}^{ch} was found to reproduce quite well the overall E_{int}, the $E_{int}^{ch} - E_{int}$ values ranging from -10 to -50 kJ mol^{-1}.

Let us now discuss the electronic spectra calculated by the CS INDO SCI procedure (see section 3.1.2) using the above-described ion pair structures. Preliminarily, we will analyze the nature of the highest occupied and lowest unoccupied MOs of primary importance in the description of the visible absorption regions where the alterations stressed in the experimental part (section 2) occur. As will be shown, the essentials of these features can be accounted for in terms of one-electron excitations from the two highest occupied to the two lowest unoccupied MOs. A general characteristic of the ion pair MOs is that they turn out to be localized either on the cation or on the anion, thus suggesting that no substantial interchromophore interactions traceable to orbital overlap[29] are operative in this case. In particular, in all cases considered, the highest occupied MO (H) is a π orbital localized on the anion having the same characteristics as the H orbital of the isolated anion. The H−1 (π) orbital on the other hand, is localized on the cation and corresponds to the H orbital of the isolated cation. In like manner, the two lowest unoccupied π^* MOs, L and L+1, are localized on the cation and the anion, respectively, and correspond to the L orbitals of the two isolated species. According to this classification, the four ion-pair orbitals H−1, H, L, L+1 will be hereafter named C, A, C*, and A*. These characteristics of the CS INDO MOs are, qualitatively speaking, independent of the semiempirical all valence electron Hamiltonian and are shared, in particular, by the MOs of the ZINDO/S method[30] which, like CS INDO, is parametrized to give UV spectra. Now, the ZINDO/S method (unlike CS INDO) is implemented in HyperChem. This enabled us to exploit the HyperChem graphical capabilities to obtain tridimensional representations of the ion-pair MOs. Figure 11 shows as an example such representations for C, A, C*, and A* orbitals of the S1 **a** type structure.

Using this four-orbital basis set, one can set up two locally excited (LE) HOMO−LUMO configurations ([A,A*], [C,C*]) and two CT ([A,C*], [C,A*]) configurations. The first CT [A,C*] and the two LE singlet configurations play a leading role in the interpretation of the emission and visible absorption properties, while the second high energy CT configuration [C,A*] is not of interest in that respect. Importantly, if the two LE configurations have almost the same energies, as happens in S1 and S2 ion pairs, resonance interactions will occur leading

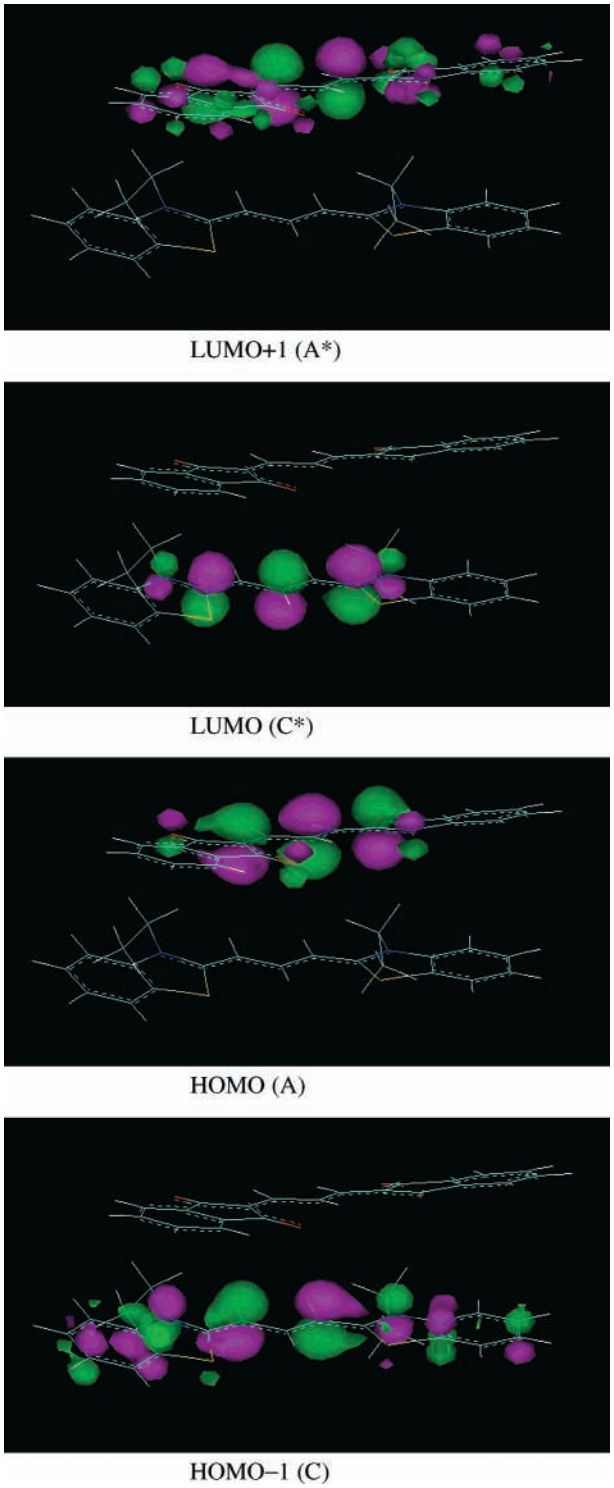

Figure 11. Display of the two highest occupied and two lowest unoccupied MOs of S1 contact ion pair with parallelly arranged components. The notations C (C*) and A (A*) refer to the localization of the MOs on the cation and the anion, respectively.

to two exciton-like states:

$$\Psi' = c_1'[\mathrm{A,A^*}] + c_2'[\mathrm{C,C^*}],\ (c_1' \cong c_2') \qquad (2)$$

$$\Psi'' = c_1''[\mathrm{A,A^*}] - c_2''[\mathrm{C,C^*}],\ (c_1'' \cong c_2'') \qquad (3)$$

According to the exciton theory for loosely bounded dimers,[31] **a** type parallel arrangements of the two chromophores are expected to give rise to substantial exciton splittings depending on the size of the local transition dipole moments. In this case, the transition from the ground state to the lower state Ψ' is forbidden while the transition to the upper state Ψ'' is strongly allowed, due to an out-of-phase and an in-phase transition dipole interaction, respectively. On the contrary, vanishing exciton splitting and comparable intensities of the $S_0-{}^1\Psi'$ and $S_0-{}^1\Psi''$ transitions should be expected to occur with **b** type orthogonal arrangements. Of course, the above model does not apply to the ion pair S3 where the two LE configurations have markedly different energies.

A deviation from this very simple three-configuration model came from the fact that other anion LE configurations, precisely [A,A*+1] and [A,A*+2], were theoretically predicted to lie at rather low energies so that they might mix with Ψ'' exciton states. This happened in particular, in the **a** type structure of S1, that will require a little more sophisticated interpretation (see below).

Bearing in mind the above considerations, let us discuss the CS INDO SCI calculation results reported in Tables 3−5, concerning transition energy (ΔE), oscillator strength (f), and nature of the first five singlet−singlet electronic transitions of S1, S2, and S3 with both **a** and **b** type structures. All the calculated spectra are characterized by the presence of a forbidden CT state at very low energy due to the one electron excitation from the HOMO, localized on the anion, to the LUMO, localized on the cation. Interestingly, this common feature is in agreement with the emission spectra in toluene solution (section 2.3), from which clearly emerged that all three contact ion pairs are not fluorescent. Such a fluorescence quenching is a well-known phenomenon occurring whenever π-electron-donating and π-electron-accepting units are put next to each other in a supramolecular architecture so as to give rise to low energy CT excited states.[32−34] In refs 32−34, where the individual components of the supramolecular system (rotaxanes, catenanes) absorb in the UV region, the formation of CT excited states was also stressed by the appearance of broad and weak bands in the visible region. In our special supramolecular systems, whose individual components absorb in the visible region, the CT bands are not surprisingly predicted to appear in the near-infrared region (Tables 3−5). This prediction, however, could not be verified experimentally: no absorption band was positively observed to come out of the baseline noise, likely because of the combined low transition probability and low ion-pair solubility in toluene. In any case, apart from a general spectral shift, the photophysical behavior of the mixed dyes under study is the same as that described in refs 32−34 for the noncovalently bonded components of rotaxanes and catenanes.

As was to be expected, the calculation results concerning the upper excited states were found to be significantly dependent on the characteristics (resonant or nonresonant) of the two components as well as on their spatial arrangement (***a*** or ***b*** type). First, let us consider the resonant ion pairs (S1 and S2), beginning from the S2 spectrum whose theoretical description (Table 4) fits the simple exciton model quite well. In fact, Table 4 shows that the calculated spectra of both **a** and **b** type structures of S2 are dominated by the presence of the two exciton states (Ψ' and Ψ'') generated by the resonance interaction of [C,C*] and [A,A*] configurations. As expected, the **a** type structure is characterized by a very large exciton splitting (0.59 eV) which is reduced to less than a half in the **b** type structure. Moreover, in the **a** type structure, the $S_0-{}^1\Psi'$ transition has forbidden character ($f < 0.1$) while the $S_0-{}^1\Psi''$ transition is most intense ($f \cong 5$, i.e., about twice the average

TABLE 3: Calculated S_0-S_n Spectra of Both Parallel (a Type) and Orthogonal (b Type) Arrangements of the S1 Ion Pair

structure	transition	ΔE (eV)	f	major excited-state configurations	assignment
a type	S_0-S_1	1.09	0.000	[A,C*] (~100%)	CT
	S_0-S_2	2.54	0.076	[C,C*] (56%), [A,A*] (38%)	Ψ'
	S_0-S_3	2.89	1.387	[A,A*+1] (25%), [A,A*+2] (30%), [C,C*] (21%), [A,A*] (17%)	LE ($+\delta\Psi''$)
	S_0-S_4	2.94	0.341	[A,A*+1] (32%), [A,A*+2] (55%)	LE
	S_0-S_5	2.97	1.531	[C,C*] (16%), [A,A*] (37%), [A,A*+1] (34%)	$\Psi''+(\delta$LE)
b type	S_0-S_1	1.25	0.000	[A,C*] (~100%)	CT
	S_0-S_2	2.57	1.707	[C,C*] (58%), [A,A*] (36%)	Ψ'
	S_0-S_3	2.73	1.365	[C,C*] (30%), [A,A*] (54%)	Ψ''
	S_0-S_4	2.94	0.277	[A,A*+1] (79%)	LE
	S_0-S_5	3.01	0.696	[A,A*+2] (75%)	LE

TABLE 4: Calculated S_0-S_n Spectra of Both Parallel (a Type) and Orthogonal (b Type) Arrangements of the S2 Ion Pair

structure	transition	ΔE (eV)	f	major excited-state configurations	assignment
a type	S_0-S_1	1.56	0.004	[A,C*] (99%)	CT
	S_0-S_2	2.25	0.065	[C,C*] (36%), [A,A*] (57%)	Ψ'
	S_0-S_3	2.44	0.043	[A,A*+1] (87%),	LE
	S_0-S_4	2.59	0.020	[A,A*+2] (88%)	LE
	S_0-S_5	2.84	5.143	[C,C*] (55%), [A,A*] (38%)	Ψ''
b type	S_0-S_1	1.36	0.000	[A,C*] (~100%)	CT
	S_0-S_2	2.59	1.344	[C,C*] (23%), [A,A*] (72%)	Ψ'
	S_0-S_3	2.83	2.914	[C,C*] (71%), [A,A*] (23%)	Ψ''
	S_0-S_4	3.15	0.151	[A,A*+2] (74%)	LE
	S_0-S_5	3.19	0.175	[A,A*+1] (73%)	LE

TABLE 5: Calculated S_0-S_n Spectra of Both Parallel (a Type) and Orthogonal (b Type) Arrangements of the S3 Ion Pair

structure	transition	ΔE (eV)	f	major excited-state configurations	assignment
a type	S_0-S_1	0.95	0.001	[A,C*] (~100%)	CT
	S_0-S_2	2.37	0.367	[C,C*] (71%), [A,A*] (22%)	Ψ'(LE)
	S_0-S_3	2.82	3.135	[C,C*] (22%), [A,A*] (66%)	Ψ''(LE)
	S_0-S_4	2.97	0.097	[A,A*+1] (84%)	LE
	S_0-S_5	2.99	0.034	[A,A*+2] (89%)	LE
b type	S_0-S_1	1.32	0.001	[A,C*] (99%)	CT
	S_0-S_2	2.46	1.495	[C,C*] (86%)	LE
	S_0-S_3	2.64	1.437	[A,A*] (86%)	LE
	S_0-S_4	2.85	0.230	[A,A*+1] (87%)	LE
	S_0-S_5	2.93	0.220	[A,A*+2] (89%)	LE

oscillator strength of the S_0-S_1 transitions of the component ions). In the pseudo orthogonal **b** type structure, on the other hand, the overall intensity is found to be distributed on both the $S_0-{}^1\Psi'$ and $S_0-{}^1\Psi''$ transitions, the oscillator strength of the first one being about a half that of the second one. As for **b** type structure of S2, it is also to be noted that (i) both exciton states Ψ' and Ψ'' are above the S_1 (H−L) states of the individual dyes (see Table 4 and Tables 1 and 2) and (ii) the weights of the two locally excited H−L configurations are quite different, [A,A*] and [C,C*] being predominant in Ψ' and Ψ'', respectively. Point i can be explained within the exciton theory. In fact, it is attributable to the fact that in this case the energies of the local excitations in the contact ion pair are higher than the excitation energies of the isolated components and that this origin shift is on the average larger than the exciton coupling term (for a detailed discussion, see ref 11). Point ii, on the other hand, indicates that the origin shifts of the two local excitations are appreciably different, so that the original "degeneracy" of the cation and anion H−L excitations (Tables 1 and 2) is removed in the associated form where the [C,C*] configuration lies at higher energy than the [A,A*] configuration. Something similar occurs also for the parallel type arrangement. In this case, however, the origin shifts are both small with respect to the exciton coupling term and hence both energies and compositions of the states Ψ' and Ψ'' conform better to the elementary version of the exciton model. Last, according to Table 4 the anion localized [A,A*+1] and [A,A*+2] configurations should play a negligible role in the visible absorption region independently of the ion pair structure.

The results of Table 3, concerning the spectrum of S1, present some specific differences with respect to those of Table 4 as far as the characteristics of the Ψ' and Ψ'' states are concerned. First of all, due to interaction with the [A,A*+1] and [A,A*+2] configurations, the higher energy exciton state Ψ'' splits into two nearby components ($\Delta E \approx 0.08$ eV) giving rise to transitions of comparable high intensities (S_0-S_3, S_0-S_5). Moreover, an anion localized transition of moderate intensity (S_0-S_4) appears between the two S_0-S_3 and S_0-S_5 transitions. Thus, in practice the overall intensity of the $S_0-{}^1\Psi''$ transition turns out to be distributed on three very little spaced transitions, so despite the apparent complexity the calculated spectrum is similar to that obtained for the **a** type structure of S2. As for the **b** type structure, the Ψ' and Ψ'' characteristics (little energy splitting, comparable intensities of the $S_0-{}^1\Psi'$ and $S_0-{}^1\Psi''$ transitions, similar contributions of the [A,A*] and [C,C*] configurations to Ψ' and Ψ'' wave functions) conform to the exciton model for orthogonally oriented transition dipoles better than do Ψ' and Ψ'' states in **b** type structure of S2 (Table 4). Among other things, in this case the state splitting is almost symmetrical with respect to the mean H−L transition energies of the individual components (Tables 1 and 2), thus suggesting negligible origin shifts.

Finally, let us examine the contact ion pair S3 (Table 5). Briefly, due to the rather different H−L transition energies of the individual components (C2 and A1F) exciton coupling plays a minor role. This is especially true for the **b** type structure where the states S_2 and S_3 are well represented by the [C,C*] and [A,A*] configurations, respectively, and the S_0-S_2 and S_0-S_3 transitions have energies and intensities fairly close to those of the S_0-S_1 transitions of the separated chromophores (Tables 1 and 2). A certain exciton coupling, however, occurs in the **a** type arrangement. This is evidenced by an increased spacing of the S_2 (mainly [C,C*]) and S_3 (mainly [A,A*]) states with respect to that of the individual S_1 states (Tables 1 and 2) and by an appreciable growth of the S_0-S_3 transition intensity at the expense of that of the S_0-S_2 transition.

Now, we need only try to explain the alterations of the visible absorption spectra of S1, S2, and S3, associated with changing

from acetonitrile to toluene solution (Figures 1−3), in terms of the theoretical descriptions provided by Tables 1 and 2 and Tables 3−5 for the individual components and the contact ion pairs, respectively. Briefly, we recall that in the dissociating solvent (acetonitrile) the visible spectra of S1 and S2 consist of a single intense band due to the superimposed color bands of the component dyes, while that of S3 exhibits two distinct bands: a band at 568 nm due to A1F and another more intense band at 648 nm due to C2 (Figure 2). All of these bands were clearly assigned to the H−L excitations localized on the component dyes (Tables 1 and 2, section 3.1.1). In the nonpolar associating solvent (toluene) the visible spectra of the three mixed dyes undergo more or less dramatic changes ranging from appearance of new bands in S1 and S2 to alteration of the relative intensities in S3 (Figures 3 and 4). In the case of S1, the spectrum in toluene exhibits two rather broad bands of similar intensities with maxima at 566 nm (near the absorption maxima of the individual dyes) and 527 nm (new band). The calculation (Table 3) does not allow a clear-cut explanation of such observations in term of only the **a** type or the **b** type S1 structure. As a matter of fact, the comparable intensity of the bands indicates a substantial involvement of the **b** type structure, but the appreciable separation of the maxima and the band broadness suggest that significant percent of parallelly arranged ion pairs should be also present in keeping with the results of the MD simulation. Further contribution at the longest wavelength band may come from the presence of solvent-separated ion pairs and/or solvated ions evidenced by the fluorescence emission and excitation spectra (Figure 6).

As for S2, the spectrum in toluene solution presents a new intense band at 598 nm and a very broad shoulder starting from the absorption region of the color band in acetonitrile (around 650 nm). With reference to Table 4, this behavior can be clearly explained by a predominance of the **a** type arrangement of the two chromophores, as suggested by the MD simulations. In fact, in agreement with the experiment the calculated spectrum of the **a** type structure is characterized by a single most intense transition (S_0-S_5), to the blue of the H−L transitions of C2 and A2 (Tables 1 and 2), associated with the upper exciton state $^1\Psi''$. The weak transitions from the ground state to the lower exciton state $^1\Psi'$ (S_2) and to the S_3, S_4 anion LE states may reasonably account for the broad shoulder extending from 650 to over 700 nm. In this case too, emission and excitation spectra (Figure 6) indicate the presence of residual solvent separated ion pairs that can give rise to weak absorptions in this region. No appreciable involvement of ***b*** type ion pairs need be invoked to explain the S2 spectrum in toluene.

Last, let us consider S3. Comparison between Figure 4, curve b, and Figure 2, curve e, shows that changing from acetonitrile to toluene solution has no significant effect on the position of the two absorption maxima (except for a slightly increased spacing) but causes a striking band intensity reversal. Although MD simulations have privileged the **b** type structure, Table 5 shows that the observed intensity effects are explainable only by a prevalence of **a** type arrangements enabling the [C,C*] and [A,A*] configurations to interact moderately. Such a contrast with the structural predictions may be explained by the fact that the calculated energy difference between the two structure is so small ($\sim$3 kcalmol^{-1}) that solvent effects neglected in our MD investigation might upset the result.

To sum up, apart from a general overestimation of the excited-state energies for both individual ions and ion pairs, the above-discussed theoretical results demonstrate that the unusual absorption and emission properties of cyanine-oxonol mixed dyes in low polarity solvents are traceable to extensive formation of contact ion pairs. The most peculiar alterations, occurring when the two dyes have superimposed color bands (resonant ion pairs), derive from more or less strong exciton coupling involving the one-electron H−L transitions localized on the two paired chromophores. In all contact ion pairs the fluorescence of the separate components is efficiently quenched by the presence of a lowest lying anion → cation CT excited state.

4. Summary and Conclusions

Within a general interest toward aggregation phenomena in polymethine dyes (cyanines, oxonols, merocyanines) and their effects on the spectroscopic and photophysical properties, in this work we dealt with the study, both experimental and theoretical, of ion-pair association in low polarity media of cyanine-oxonol mixed dyes. Starting from spectroscopic evidence previously reported in the literature, we reappraised the subject in order to search into the theoretical aspects of the observed phenomena. For this purpose, we built three model mixed dyes combining, two by two, two vinylogous cyanines (thiacarbo- and thiadicarbocyanine; C1 and C2) and two corresponding oxonols (A1/A1F, A2) in such a way as to obtain two systems (S1, C1−A1, and S2, C2−A2) whose components have almost superimposed color bands and a system (S3: C2−A1F) whose components absorb in quite far spectral regions. Absorption and emission properties of these systems as well as of salts formed by the individual chromophores with colorless counterions were investigated both in acetonitrile and in toluene solution in order to analyze the effects of ion-pair association. In the low-polarity solvent, where contact ion pairing is expected to occur, the absorption spectra of S1 and S2 were characterized by the appearance of a new intense band to the blue of the absorption region of the individual chromophores. In the latter region, the S1 spectrum exhibited a second band of similar intensity while that of S2 presented only a very broad shoulder. On the other hand, the absorption spectrum of S3 in toluene differed from that in acetonitrile only for the relative intensities of the two distinct C2 and A1F absorption bands. As far as fluorescence properties are concerned, in toluene solution the three investigated systems exhibited emissions much weaker than in acetonitrile attributable to residual solvent-separated ion pairs, while the contact ion pairs were found to be nonfluorescent.

The theoretical interpretation of this peculiar behavior was based on extensive calculations of structures and electronic spectra of individual chromophores and contact ion pairs. The ion pair structures were determined combining MD calculations with local full geometry optimizations at the PM3 level. Such a procedure led two structures being localized of comparable energies differing from one another by the arrangement (parallel or orthogonal) of the long molecular axes. The distance between the molecular planes ranged between 3.4−3.6 Å for S1 and S2 and $\sim$4 Å for S3.

The electronic spectra of these bichromophoric complexes were calculated at the CS INDO SCI level. The localization of the molecular orbitals on the chromophoric subunits enabled us to interpret the calculation results in terms of local and charge-transfer excitations. In systems S1 and S2, where the HOMO−LUMO excitations of the two ions have about the same energies, we found large exciton effects, due to interaction of the H−L transitions localized on the two chromophoric units, which reproduced quite well the most striking alterations observed on changing from the highly polar to the little polar solvent. Calculations suggested the prevalence of parallelly

arranged ion pairs for the system S2, but comparably high contributions from both parallel and orthogonal type structures in the case of the S1 system. A moderate exciton effect due to the presence of parallel type arrangements had also to be invoked to explain the intensity modifications characterizing the spectrum of S3 in toluene solution. Moreover, calculations showed that the peculiar emission properties exhibited by the three mixed dyes in low-polarity solvents are traceable to the charge-transfer nature of the lowest excited singlet state in the three *contact* ion pairs.

Acknowledgment. Research jointly supported by the MURST (Roma) and the University of Modena and Reggio Emilia within the "Programmi di Ricerca di Interesse Nazionale". Dr. Zh. A. Krasnaya is warmly thanked for the gift of the dyes studied. Dr. M. Caselli's collaboration with some of the fluorescence experiments is gratefully acknowledged.

References and Notes

(1) *The Theory of the Photographic Process*, 4th ed.; James, T. H., Ed.; Macmillan: New York, 1977.

(2) Schäfer, F. P.; in Schäfer, F. P., Ed.; *Dye Lasers*, *Topics in Applied Physics 1*; 3rd ed.; Springer-Verlag: Berlin, 1990.

(3) Prasad, P. N.; Williams, D. J. *Introduction to Non-Linear Optical Effects in Molecules and Polymers*; Wiley: New York, 1991.

(4) Khazraji, A. C.; Hotchandani, S.; Das, S.; Kamat, P. V. *J. Phys. Chem. B* **1999**, *103*, 4693.

(5) Yamazaki, I.; Tamai, N.; Yamazaki, T.; Murakami, A.; Mimuro, M.; Fujita, Y. *J. Phys. Chem*. **1988**, *92*, 5035.

(6) Fabian, J.; Hartmann, H. *Light Absorption of Organic Colorants*; Springer: Berlin, 1980; Chapter 12.

(7) Griffiths, J. *Colour and Constitution of Organic Molecules*; Academic Press: London, 1976.

(8) Momicchioli, F.; Baraldi, I.; Berthier, G. *Chem. Phys*. **1988**, *123*, 103. Momicchioli, F.; Ponterini, G. *Chem. Phys*. **1991**, *151*, 111. Baraldi, I.; Carnevali, A.; Caselli, M.; Momicchioli, F.; Ponterini, G.; Berthier, G. *J. Mol. Struct*. (*Theochem*) **1995**, *330*, 403. Baraldi, I.; Carnevali, A.; Momicchioli, F.; Ponterini, G.; Berthier, G. *Gazz. Chim. Ital*. **1996**, *126*, 211. Tatikolov, A. S.; Derevyanko, N. A.; Ishchenko, A. A.; Baraldi, I.; Caselli, M.; Momicchioli, F.; Ponterini, G. *Ber Bunsen-Ges. Phys. Chem*. **1995**, *99*, 763.

(9) (a) Momicchioli, F.; Baraldi, I.; Ponterini, G.; Berthier, G. *Spectrochim. Acta* **1990**, *46A*, 775**.** (b) Baraldi, I.; Carnevali, A.; Momicchioli, F.; Ponterini, G. *Spectrochim. Acta* **1993**, *49A*, 471.

(10) Baraldi, I.; Ghelli, S.; Krasnaya, Zh. A.; Momicchioli, F.; Tatikolov, A. S.; Vanossi, D.; Ponterini, G. *J. Photochem. Photobiol. A*: *Chem*. **1997**, *105*, 297. Baraldi, I.; Momicchioli, F.; Ponterini, G.; Vanossi, D. *Chem. Phys*. **1998**, *238*, 353; *Adv. Quantum Chem*. **1999**, *36*, 121.

(11) Millié, P.; Momicchioli, F.; Vanossi, D. *J. Phys. Chem*. B **2000**, *104*, 9621.

(12) Ponterini, G. *Chem. Phys*. **1997**, *216*, 193.

(13) Tatikolov, A. S.; Ishchenko, A. A.; Ghelli, S.; Ponterini, G. *J. Mol. Struct*. **1998**, *471*, 145.

(14) Tatikolov, A. S.; Ponterini, G. *J. Photochem. Photobiol. A*: *Chem*. **1998**, *117*, 35.

(15) Ishchenko, A. A. *Russ. Chem. Rev*. **1991**, *60*, 865.

(16) Malhotra, S. S.; Whiting, M. C. *J. Chem. Soc*. **1960**, 3812.

(17) HyperChem. *Computational Chemistry Manual*; Hypercube, Inc.: Gainesville, Florida, 1996.

(18) Stewart, J. J. P. *J. Comput. Chem*. **1989**, *10*, 221.

(19) Momicchioli, F.; Baraldi, I.; Bruni, M. C. *Chem. Phys*. **1983**, *82*, 229.

(20) Krasnaya, Zh. A.; Stytsenko, T. S.; Gusev, D. G.; Prokof'ev, E. P. *Izv. AN SSSR* (*Russ. Bull. Acad. Sci. SSSR Div. Chem. Sci*.) **1986**, 1596.

(21) Krasnaya, Zh. A.; Stytsenko, T. S.; Bogdanov, V. S.; Monich, N. V.; Kul'chitskii, M. M.; Pazenok, S. V.; Yagupol'skii, L. M. *Izv. AN SSSR* (*Russ. Bull. Acad. Sci. SSSR Div. Chem. Sci*.) **1989**, 636.

(22) Isak, S. J.;.Eyring, E. M. *J. Phys. Chem*. **1992**, *96*, 1738.

(23) Del Re, G. *Theor. Chim. Acta* **1963**, *1*, 188.

(24) For a review on the Del Re method and its structural applications, see: Barbier, C.; Berthier, G. *Adv. Quantum Chem*. **1999**, *36*, 1.

(25) Mataga, N.; Nishimoto, K. *Z. Phys. Chem*. **1957**, *12*, 335; **1957**, *13*, 140.

(26) Etter, M. C.; Kress, R. B.; Bernstein, J.; Cash, D. J. *J. Am. Chem. Soc*. **1984**, *106*, 6921.

(27) Atkins, P. W.; Friedman, R. S. *Molecular Quantum Mechanics*, 3rd ed.; Oxford University Press: 1997; Chapter 9.

(28) Claverie, P. *Intermolecular Interactions: from Diatomic to Biopolymers*; Pullman, B., Ed.; Wiley: New York, 1975.

(29) Cornil, J.; dos Santos, D. A.; Crispin, X.; Silbey, R.; Brédas, J. L. *J. Am. Chem. Soc*. **1998**, *120*, 1289.

(30) Ridley, J.; Zerner, M. C. *Theor. Chim. Acta* **1973**, *32*, 111. Ridley, J.; Zerner, M. C. *Theor. Chim. Acta* **1976**, *42*, 223.

(31) Kasha, M.; Rawls, H. R.; Ashraf El-Bayoumi, M. *Pure Appl. Chem*. **1965**, *11*, 371.

(32) Anelli, P. L.; Ashton, P. R.; Ballardini, R.; Balzani, V.; Delgado, M.; Gandolfi, M. T.; Goodnow, T. T.; Kaifer, A. E.; Philp, D.; Pietraszkiewicz, M.; Prodi, L.; Reddington, M. V.; Slawin, A. M. Z.; Spencer, N.; Stoddart, J. F.; Vincent, C.; Williams, D. J. *J. Am. Chem. Soc*. **1992**, *114*, 193.

(33) Ashton, P. R.; Ballardini, R.; Balzani, V.; Credi, A.; Gandolfi, M. T.; Menzer, S.; Pérez-García, L.; Prodi, L.; Stoddart, J. F.; Venturi, M.; White, A. J. P.; Williams, D. J. *J. Am. Chem. Soc*. **1995**, *117*, 11171.

(34) Asakawa, M.; Ashton, P. R.; Ballardini, R.; Balzani, V.; Belohradský, M.; Gandolfi, M. T.; Kocian, O.; Prodi, L.; Raymo, F. M.; Stoddart, J. F.; Venturi, M.; *J. Am. Chem. Soc*. **1997**, *119*, 302.